

# Using a physics-based reflection model to study the reddening effect observed in spectrometric measurements of artificial space objects

**Major Donald Bédard**

*Royal Military College of Canada, Department of Physics*

*Email: donald.bedard@rmc.ca*

## ABSTRACT

Almost all remote spectrometric measurements obtained of artificial space objects in the last decade contained an unexpected and unexplained reddening of reflectance spectra when compared to either modelled predictions or ground truth measurements of sample spacecraft material. During the spectrometric characterization experiment of an engineering model (EM) of the CanX-1 nanosatellite, an increase of the slope of the overall reflectance curve was observed in various illumination and sensor geometries. Observation of the reddening effect such as was seen during the CanX-1 EM experiment has not been reported to have been observed in a laboratory environment before. With this in mind, a study was initiated to assess how the specular component of the spectral reflectance, from metallic surfaces and photovoltaic cells, varied as a function of changing illumination and sensor geometry. This paper presents the preliminary results of a new approach aimed at explaining the reddening effect commonly observed in remote spectrometric measurements of artificial space objects.

## 1. INTRODUCTION

Over the last decade, astronomical reflectance spectroscopy has been used - both in the US and Europe - to characterize the surface composition of artificial space objects [1], [2], [3]. Although this technique has been shown to be successful at providing insight into the compositional makeup of the observed objects, more work remains to be done before this technique can be considered an operational capability. One question that remains unanswered concerns the unexpected increase in reflectance at wavelengths greater than 600 nm that has been observed in measurements of all observed objects except for one class of space debris, namely spent Inertial Upper Stage (IUS) rocket bodies [2], [4].

In late 2010, a (lab-based) spectrometric characterization of an engineering model (EM) for the CanX-1 cubesat was conducted with the aim of validating a spectral reflectance collection procedure before it was actually attempted on a flight-ready spacecraft, in this case the NEOSSat spacecraft, a mission currently manifested for launch in the first half of 2012. To the surprise of the experimenters, the apparent reddening effect, which has never been reported to have been observed in a laboratory environment, was seen on numerous occasions during the experiment.

As a result of the CanX-1 EM experiment, it was determined that a thorough understanding of reflectance spectroscopy on artificial space objects could only be achieved through an in-depth analysis of how sunlight is reflected from typical spacecraft surfaces. This paper presents the initial findings of a study that is aimed at explaining the reddening effect commonly observed in remote spectrometric measurements of artificial space objects. The approach was focused on examining if and how the spectral content of specular reflections changes with varying incident light angles.

The paper begins with a brief review of the reddening effect as it is seen in the remote spectrometric data followed by a discussion of how it was observed during the CanX-1 EM characterization experiment. The discussion then describes the considerations that led to the belief that the unexplained reddening effect may in fact be a natural physical phenomenon that has been unaccounted for in both how the ground-truth measurements are collected and in the spectrometric measurement prediction tools that are currently used. Next, the paper presents the modelling (in MATLAB) that was conducted to determine whether the spectral content of the specular reflectance varied with changes in the illumination geometry. The paper continues with an analysis of the results and concludes with a summary of the research activities that will continue in the upcoming months.

## 2. REDDENING OF REMOTE SPECTRA

In 2000, as part of her doctoral research, Jorgensen [5] proposed that remote spectroscopy could be used to characterize artificial space objects into three broad categories: metals, plastics and paints. Her doctoral work consisted of obtaining and analyzing, in a controlled laboratory environment, spectrometric measurements of materials commonly used on spacecraft. For each material, the spectral reflectance consisted in an average of approximately 10 measurements all taken in the same illumination-object-sensor geometry. It is important to note that the effect of varying this geometry on the measured spectral reflectance for each material was not considered during this study. Nonetheless, by 2001 her efforts resulted in a database containing over 300 types of material commonly found on the surface of satellites [1].

Remote spectrometric measurements of active satellites and space debris were subsequently acquired with the AFRL Maui Optical Site (AMOS) 1.6-meter telescope equipped with the Spica spectrograph [1]. The method used to identify the material types of the artificial space objects consisted of matching the various spectral features, as well as the overall reflectance curve, of the remote measurements to the laboratory samples. This method successfully demonstrated that artificial space objects could be characterized according to the material type. However, with the exception of spent IUS rocket bodies, all remote spectrometric measurements of artificial space objects collected by Abercromby *et al.* in the last 10 years show an increase in the slope of the reflectance curve as the wavelengths increased beyond approximately 600 nm [2]. This phenomenon was termed ‘reddening’ and has been defined as an ‘*increase in the slope of the reflectance as the wavelength increases.*’

Even if no definitive physical process has been identified as the source of variation in spectral reflectance, space weathering is currently the leading contender as to the cause behind the reddening effect [6]. Space weathering is a term widely used by the asteroid community to describe how the space environment modifies the spectral reflectance of asteroids [7]. This process, which alters the reflectance spectra over astronomical time scales, includes irradiation by cosmic and solar wind particles as well as bombardment by interplanetary dust.

Notwithstanding, traits with respect to the reddening effect have been identified. First, Abercromby *et al.* have showed that matching features and slope of the reflectance curves below 600 nm was possible [1]. Second, remote spectrometric observations conducted a few weeks after the launch of the six FORMOSAT-3 spacecraft, which were all characterized before their launch, already showed the effects of reddening [2]. This led to the conclusion that whatever the process involved, it occurs on a very short timescale. Finally, spectral reflectance measurements on returned spacecraft material conducted in a laboratory have shown no presence of reddening. This led to the conclusion that this process was reversible once the materials were exposed to the Earth’s atmosphere [6]. Although there have been numerous attempts at reconciling the models and the observed data, to date there has not been a satisfactory answer to this problem [8].

## 3. CHARACTERIZATION OF THE CANX-1 ENGINEERING MODEL

During a Canadian experiment focussed on the spectrometric characterization of the CanX-1 EM (Fig. 1), a flight prototype of the actual CanX-1 spacecraft, it was observed that spectral reflectance varied greatly when the position of the light source and the detector, with respect to the surface normal, were changed. The CanX-1 EM characterization experiment is described in more details in another paper in these proceedings.

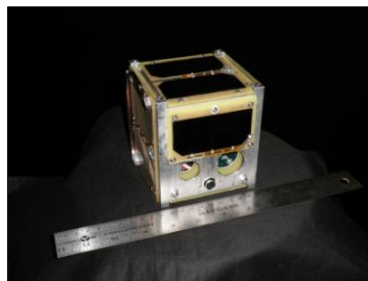


Fig. 1. The CanX-1 EM is a 10 x 10 x 10 cm nanosatellite prototype designed, built and launched by the University of Toronto Space Flight Laboratory in 2003 [9].

Variations in the magnitude of the detected spectral reflectance had been expected; the experimenters had not, however, anticipated that the slope and the spectral content (i.e. the overall shape of the reflectance curve) between 350 and 2500 nm would change as the illumination and sensor geometry varied. Although the displacement of various spectral features was rapidly attributed to thin film interference caused by the solar cells, the increase in reflectance beginning in the region of 800 nm in certain illumination-sensor geometries remained unexplained. It was later uncovered that this phenomenon, clearly seen in Fig. 2, was commonly observed in spectral reflectance obtained from remote observations and was referred to as the reddening effect. To date, it has not been reported having been observed before in a laboratory environment.

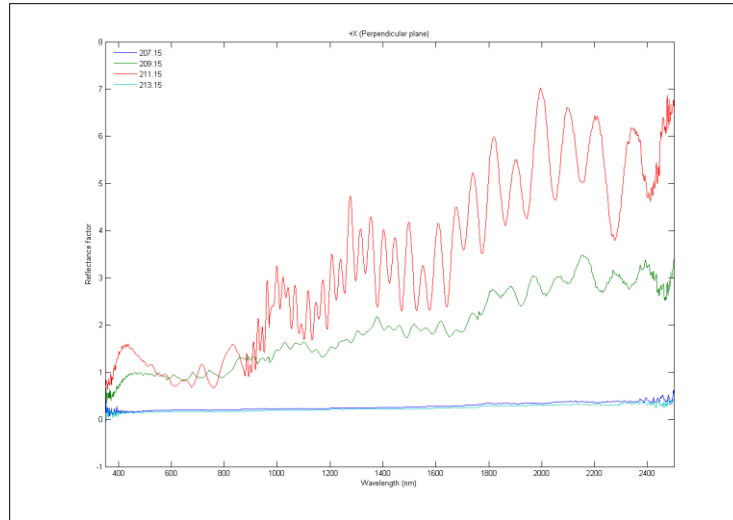


Fig. 2. Observed reddening of the spectral reflectance as the spectrometer moved towards the specular reflection, which is shown by the red line.

A careful review of the experimental procedure was conducted to determine if there was mishandling of the spectrometer used during the characterization of the CanX-1 EM. Although minor errors were noted, there were none that could have affected the measurements themselves. Following a review of the limited literature available on the subject of spectral reddening for artificial space objects, the question was posed as to whether the reddening effect was a natural consequence unaccounted for in both how the ground truth measurements were collected and how the spectral reflectance model, against which the remote measurements have been compared, were devised.

To date, explanations for the reddening effect have all been directed at trying to find the physical processes that are responsible for modifying the spectral reflectance once the spacecraft is placed in Earth orbit. However, the prediction model and the ground-truth data used to predict the spectra for artificial objects have not been exposed to the same level of scrutiny.

The model used by Abercromby *et al.* to predict reflectance spectra is based on empirical spectrometric measurement collected in a controlled environment. For a particular material, measurements are collected and then averaged to provide one spectral signature for the material. This average ground-truth data is then used by the model to predict spectral reflectance. Using the orientation of the material and its position along its orbital path, the model then multiplies the averaged spectra by a term that is a function of the Sun's and sensor's position in order to modify the magnitude of the reflected energy [10], [8].

This process is based on the inherent assumption that the shape of the spectral reflectance remains constant irrespective of the illumination and sensor geometry. In other words, although the model accounts for the fact that the reflected *energy* will be greater in certain geometries, it assumes that this change in reflected energy will be *constant* for all wavelengths. With this in mind, a physics-based reflection model was used to examine this assumption by studying how spectral reflectance, from metallic surfaces and solar cells, changes as a function of a varying illumination and sensor geometry.

#### 4. UNDERSTANDING REMOTE SPECTROMETRIC MEASUREMENTS

The first step in studying this problem is to gain a better understanding of what a remote spectrometric observation of an artificial space object actually represents. In order to achieve this, a STK scenario was created in which the vector geometry tool was used to visualize and quantify how the illumination and sensor geometry varied over the course of various observation periods.

Reflectance spectroscopy of artificial space objects typically require an integration period ranging from 10 seconds for the very bright targets to 60 seconds for the relatively dimmer ones [1], [3]. As a comparison, spectral reflectance measurements taken in a controlled environment typically require an integration time of a few milliseconds in order to obtain a sufficient signal to noise ratio. Over the course of this integration period in the laboratory, the object from which the reflections are measured remains stationary with respect to the illumination source and the sensor. This not the case if that same object is placed in Earth orbit. As can be seen in Fig. 3, the position of the ground-based sensor (shown as a green vector) with respect to the illuminated surface of the spacecraft (surface normal is shown as a blue vector) varies considerably over a 10-second observation.

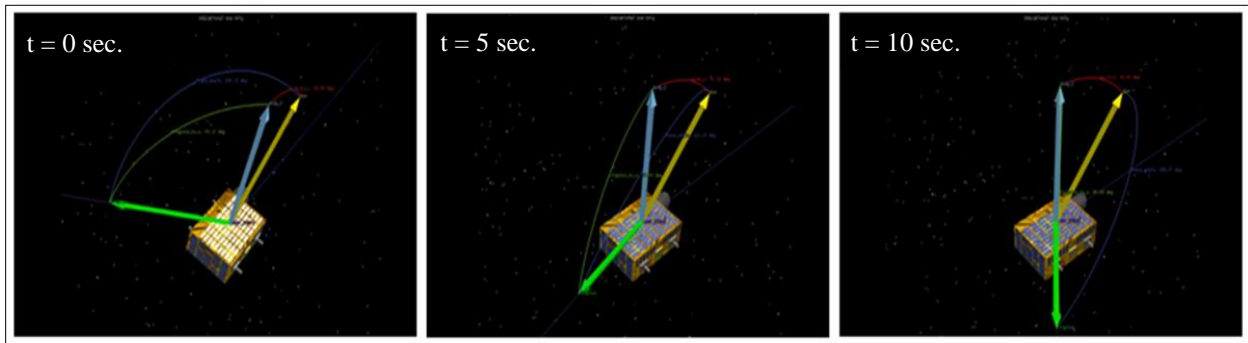


Fig. 3. A simulation showing the variation in the Sun-spacecraft-sensor geometry over the course of a 10-second exposure.

The case presented in Fig. 3 is a best-case scenario in which the spacecraft's orientation with respect to the Sun remains practically constant. In other words, the illumination incidence angle remains practically constant throughout the integration period. This situation may apply to a wide range of active satellites whose design require their solar panels to track the Sun. In less than ideal situations, the illumination geometry will vary for certain type of active satellite with the rate of change of the illumination incidence angle depending on the type of mission the spacecraft is conducting. In the case of space debris (or active spacecraft) with uncontrolled attitudes the rate of change of the illumination geometry will be random. Thus in summary, during one remote spectrometric observation, the illumination geometry will vary with a rate of change that largely depends on the type of object that is being observed. The first question that arises at this point is whether different illumination geometries will produce spectral reflectances having the same shape, i.e having the same spectral features.

The next issue to be considered by the case presented in Fig. 3 is that the arc followed by the green vector will invariably traverse up to three reflection components. In general, physics-based reflectance models stipulate that the bidirectional reflectivity ( $\rho_{bd}$ ) is composed of three components, namely the specular component ( $\rho_{sp}$ ), the directional-diffuse term ( $\rho_{dd}$ ) and the uniform-diffuse reflection ( $\rho_{ud}$ ) [11]. Mathematically, this is expressed as follows:

$$\rho_{bd} = \rho_{sp} + \rho_{dd} + \rho_{ud} \quad (1)$$

This leads to the second consideration which is that reflectance spectroscopy applied to artificial space objects is in fact a summation of spectral measurements collected on the arc travelled by the sensor. Fig. 4 is provided to provide a two-dimensional perspective of this statement. Assuming a panel consisting an homogenous material, then the second question is whether the spectral content of each of these component is constant or not.

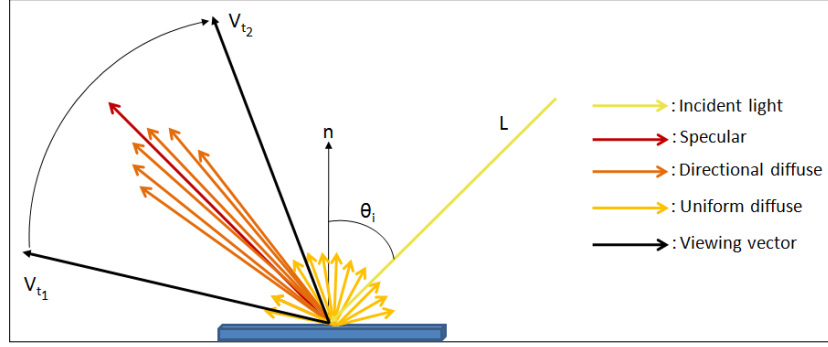


Fig. 4. In the simple case in which the object is stationary with respect to the illumination vector,  $L$ , then the viewing vector,  $V$ , travels across different components of the reflection. The sensor, continuously integrates the reflections between the observation period ranging from  $t_1$  and  $t_2$ .

This section summarized the two central questions posed by research activity aimed at studying the reddening effect. The first question is to determine whether the spectral content, or the shape of the spectral reflectance, for the various reflection components remain the same for different incident angles. The second question is whether for a given incidence angle, the shape of the spectral reflectance for the various components is the same or not. If non-negligible differences are observed in any of the two situations, then the assumption described in Section 3 will need to be revisited. Although the CanX-1 EM characterization experiment had provided a positive answer to both of these questions, it was decided to further analyze those results through modelling. The remainder of the text will describe the modelling experiment that was conducted to answer the first question. Work aimed at answering the second question is still in progress and will not be reported in this paper.

## 5. REFLECTANCE EXPERIMENT

The qualitative assessment now gives way to a modelling analysis aimed at verifying if variations in the illumination and sensor geometry can bring changes in the shape of the spectral reflectance. It is hypothesized that the reddening effect commonly observed in remote spectrometric observations, when compared to spectral measurements taken in a controlled environment, is caused by variations in the illumination and sensor geometry that are unaccounted for in both the models used to predict remote measurements as well as in the material characterization procedures that have been used up to date.

The aim of the modelling was to determine whether the spectral content of specular reflections from different incident angles was the same or different. In order to answer this question, a simplified physics-based model was implemented in a MATLAB environment.

For a perfectly smooth surface, defined as having an RMS surface roughness of zero, all incident light is reflected in the specular direction with no dispersal of the ray. It must be noted that conditions for specular reflection can also be satisfied in the case where the RMS surface roughness is different than zero if the roughness size scale is much smaller than the wavelength of the incident light being considered. Knowledge of the total ideal specular reflection from a material provides the upper limit on the reflected energy. Fresnel developed a model in which the magnitude of the ideal specular reflection depends on the index of refraction of the material,  $n(\lambda)$ , and the angle of incidence,  $\theta_i$  [12]:

$$R_{total} \theta_i, \lambda = \frac{R_{te} \theta_i, \lambda + R_{tm}(\theta_i, \lambda)}{2} \quad (2)$$

where  $R_{te}$  and  $R_{tm}$  are the reflectance for the transverse electric (TE) and transverse magnetic (TM) wave respectively. In cases when the surface is not perfectly smooth, then its RMS roughness must be taken in consideration and the specular reflectance is reduced and calculated using the following approximation [13]:

$$\rho \theta, \lambda \approx R_{total} \theta_i, \lambda e^{-(4\pi\frac{\sigma}{\lambda}\cos\theta_i)^2} \quad (3)$$

where  $\sigma$  is the RMS surface roughness of the material. The difference  $R_{total}(\theta, \lambda) - \rho(\theta, \lambda)$  is the portion of light that is scattered to the remainder of the hemisphere.

First, using equation (3), reflections from two types of surfaces were studied as part of this experiment. The first materials were metals that are commonly employed on the surfaces of spacecraft and for which complex indices of refraction were readily available in open literature. These consisted of aluminum, titanium, gold, and copper. The second type of material considered were triple junction (TJ) solar photovoltaic cells since practically all Earth-orbiting artificial space objects have these on their surface. Given that solar cells are composed of several layers of semi-conductor materials that are typically covered by a double anti-reflection layer, a separate MATLAB model was created to simulate various types of solar cells. As in the case of the metals, complex indices of refraction for the semi-conductor material within the cell were obtained from open sources.

Next, the use of color ratios, analogous to those used in astronomy, was chosen as the most efficient method to determine if the shape of the spectral reflectance varied over a range of incidence angles. Once this experimental approach was selected, an algorithm was implemented in MATLAB to evaluate the variation in spectral reflectance of reflections from metal and solar cells. Fig. 5 summarizes the algorithm that was developed and used to obtain ratios.

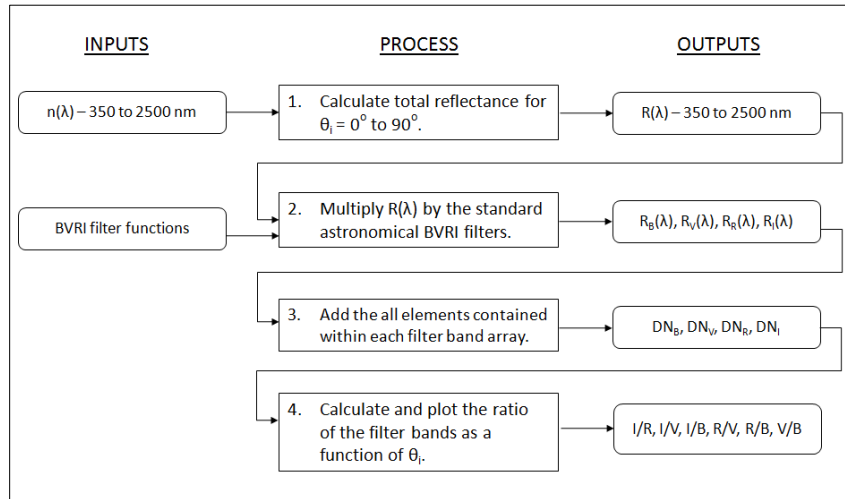


Fig. 5. Experimental process elaborated to study the variation of the spectral reflectance of the specular component.

The first step in the algorithm is to calculate the spectral reflectance between 350 to 2500 nm for a range of incidence angle ranging from  $0^\circ$  to  $90^\circ$ . For this step, two different models were used to calculate the reflectance. The first model, which is based on a theory of thin film interference, was used to calculate spectral reflection from solar cells. The model created for reflection from solar cells represents a special case and is summarized in Annex A of the paper. The second one, based on equation (3), was used to calculate the reflectance from metallic surfaces in which the RMS surface roughness could be modified.

The second step in the process was to take the spectral reflectance and multiply it by the four BVRI filter functions thereby producing four sets of reflectance files, one for each filter. The BVRI color filters were selected since these are common astronomical filters that are currently available at the Royal Military College Observatory. Hence, it was assumed that positive results in this simulation could be easily tested in an observational experiment.

The third step consisted in adding the individual elements of each of the four reflectance files thus producing a count for each color band. The product of this process emulates how an astronomical CCD camera fitted with a filter detects incoming photons from a space object. The fourth and final step in the process consisted in producing color ratio using the counts obtained in the previous step.

In all, the six color ratios provide a measure of variations in the content of the spectral reflectance in the BVRI bands. A constant ratio as a function of incidence angle would necessarily imply that the shape of the spectral reflectance within these bands doesn't vary with changes in the incidence angle, implying that the inherent assumption of the model used by Abercromby *et al.* was correct. However, if the ratios do vary as a function of incidence angle then this would signify that the overall shape of the spectral reflectance changes with variation in the illumination geometry and that the assumption will need to be revisited.

## 6. RESULTS

The first analysis was conducted using a modelled triple junction cell. Since no information was found on surface characteristics of solar cells, it was assumed that the RMS surface roughness would be zero. As shown in Fig. 6, there is significant variation of the various normalized color ratios as the angle of incidence is varied between 0 and 90°. The most significant changes are noted for the I/R, R/V and R/B ratios. In the case of the I/R ratio, the plot shows an increase of reflectance of the I-band with respect to the R-band as  $\theta_i$  increases. In the case of the R/V and R/B ratios, the graphs are interpreted as increases of reflectance in the R-band with respect to the V and B bands respectively as  $\theta_i$  increases. A visual look at any solar cell at an incidence angle of 0° clearly shows the dark blue appearance of the cells while at higher incidence angles this bluish reflection gives way to a redder reflection. In all three cases, although the analysis of the spectral variation has been limited to the specular component of the reflection, it is clearly showing that there is a reddening of the reflectance as the incidence angle is increased.

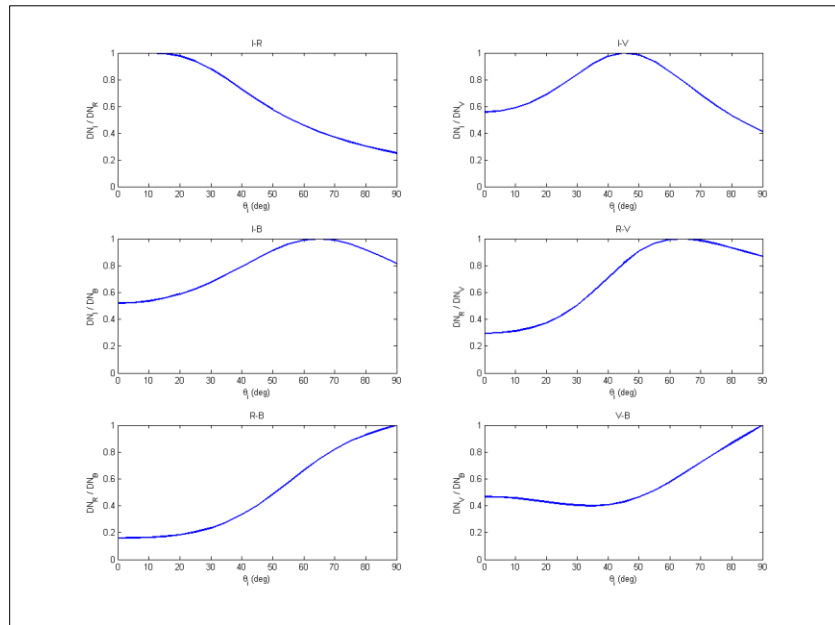


Fig. 6. Normalized color ratios for a modelled triple-junction photovoltaic cell.

Metals were considered in the second set of the experiment. For each metal, three simulations were conducted: one in which the metallic surface was assumed to be perfectly smooth, the second with an RMS surface roughness of 50 nm and the third with a roughness value of 150 nm. Unfortunately, no reliable source of information on typical RMS surface roughness for spacecraft surface material could be obtained for this experiment. Although the figures above are believed to be reasonable assumptions, confirmation of actual values will be required in the future for validation purposes.

Variations in the color ratios were observed for all four metals in the first set of simulations in which the metallic surfaces were assumed to be perfectly smooth. Results for aluminum and gold are presented in Fig. 7. Color ratios obtained for titanium surface yielded similar results to aluminum while copper closely matched those obtained for gold. For this reasons, the results for these two metals are not included as part of this paper.

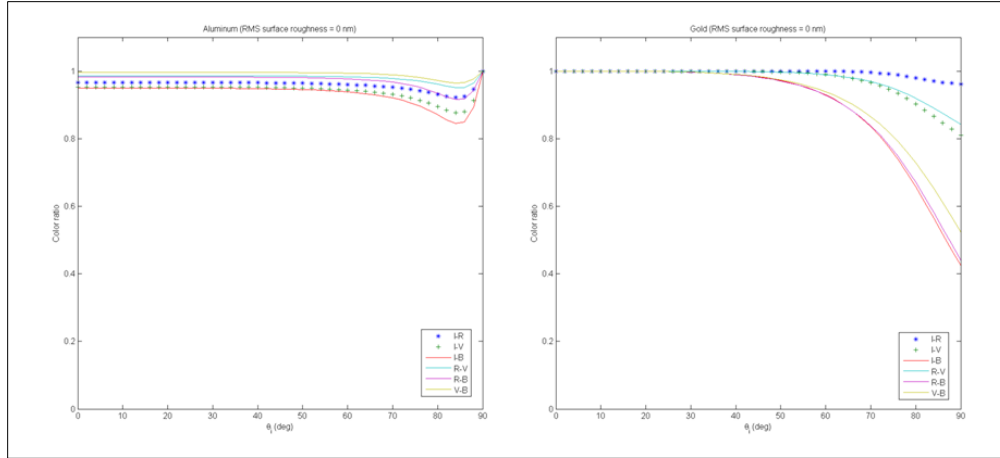


Fig. 7. Normalized color ratios for reflection from aluminum (left) and gold (right) having an RMS surface roughness of 0 nm.

As can be seen for aluminum, there is a slight variation in the color ratios between an incidence angle of approximately 70 and 90 degrees. This variation is more pronounced for gold and begins at the lesser angle of 40° of incidence. As the RMS surface roughness was increased, the variation for all metals increased significantly. An example is provided at Fig. 8.

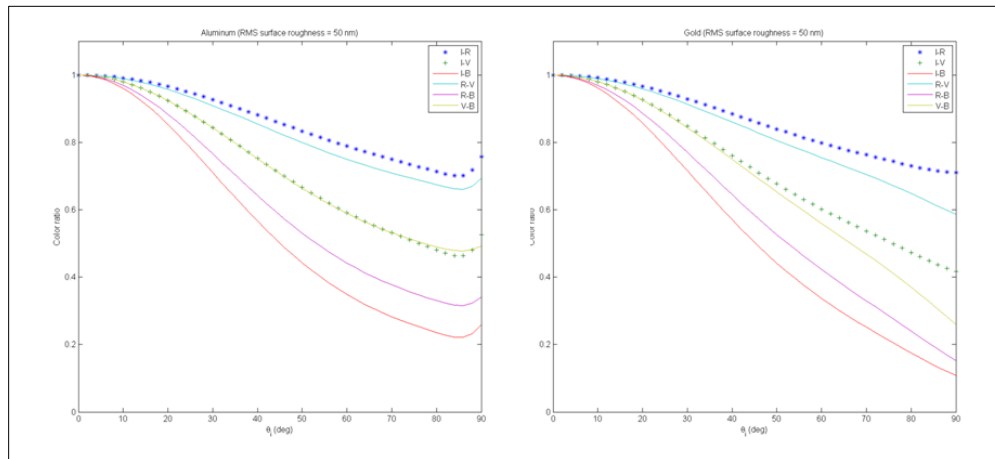


Fig. 8. Color indices for reflections from aluminum with RMS surface roughness of 50 nm.

Although this case study looked at only four metals, the first conclusion that was drawn is that there is a non-negligible variation in the spectral content of the specular component as the incidence angle is changed. When considering different types of metals, the changes in color indices showed much variability. For example, reflections from perfectly smooth gold and copper surfaces showed appreciable variation for all color indices while aluminum and titanium displayed very little changes. As the RMS surface roughness was increased, the variation in the spectral content of the reflection became more pronounced for all metallic surfaces. Therefore, it can be stated that the magnitude of the variation is dependent on the type of metal as well as its surface roughness.

In the cases where the surface roughness was different than zero, the color ratios became progressively smaller as  $\theta_i$  is varied from 0° to 90° indicating that the reflectance at the shorter wavelengths was becoming stronger when compared to the longer wavelength. At first thought this consequence appears contrary to the anticipated results seeking to explain the reddening effect. However in the context of a curve matching process, depending how the reference was selected, this variation could potentially be misinterpreted as an increase of reflectance at higher wavelength compare to lower values.

A different plot in which spectral reflectance curves were calculated for increasing values of  $\theta_i$  and graphed on the same figure shows more clearly how the surface roughness affected the reflectance at shorter wavelengths. As illustrated in Fig. 9, the shorter wavelengths are scattered in greater quantity at low incidence angles where the RMS surface roughness is greater than zero. As this angle increases, the scattering of these wavelengths becomes less pronounced to the point where it is irrelevant at  $90^\circ$ .

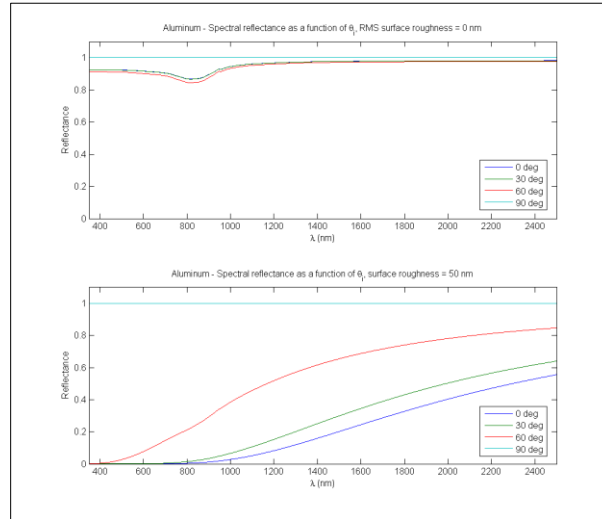


Fig. 9. Comparison of the spectral reflectance for an aluminum smooth and 50 nm RMS roughness as a function of incidence angle.

The above results show that the inherent assumption, that the shape of the spectral reflectance remains constant as the illumination and sensor geometry is changed, needs to be revised. Moreover, these results also provide initial confidence in the hypothesis that the reddening effect is caused by a previously unaccounted for variation in the illumination and sensor geometry.

Although much work remains to be done, the results seem to indicate that the reddening effect observed in the remote data has its root cause in a reduced specular reflectance of the shorter wavelengths compared to the higher ones. Two conditions are required in order to lead to this interpretation. In the first place, the ground truth data would have to be based on a limited and averaged set of measurements. Unless all the samples were taken in a geometry favouring the scattering of the short wavelengths, then any comparison would necessarily show an increase in red reflectance. The second condition is in how the remote spectrometric measurements are compared to the ground truth measurements. Currently, this comparison is achieved by matching the absorption bands and the overall reflectance curve of the measurement. This method has been identified as the first of the three “Great Mistakes” of interpreting asteroid spectra and is recommended to be used only when the observed target has strong distinct spectral features [14]. Although the curve matching method has proven useful in allowing Abercromby *et al.* to characterize hundreds of RSO, it could also be the cause of the apparent reddening effect. An in-depth analysis of the curve matching process will be required to determine if this is the case. No definitive conclusion with respect to this specific issue is affirmed at this time due to the lack of precise information on how the comparison is conducted. This is obviously one of the critical issues that will require further analysis.

The scope of this simulation was limited to studying the variation of the spectral reflectance of the specular component. In spite of the fact that a remote spectrometric observation will be not limited to a sampling of this reflection component, this experiment has demonstrated that the spectral content of the specular component varies as the incidence angle is changed. Even if this experiment has raised serious questions about the validity of the assumption that the spectral reflectance’s overall shape doesn’t change with illumination and sensor position, the question that now arises is whether the variation in spectral reflectance observed in this simulation could translate into the reddening effect commonly observed in remote spectrometric observations. This question is expected to be answered within the next year.

## 7. CONCLUSION

This paper presented the preliminary results of a new approach aimed at explaining the reddening effect commonly observed in remote spectrometric measurements of artificial space objects. To date, space weathering remains the leading contender as the cause behind this effect even if no definitive physical process has been identified. The study presented herein used a simplified physics-based reflection model to study the specular component of reflections from triple-junction photovoltaic cells as well as metallic surfaces commonly employed in spacecraft design. By multiplying the calculated spectral reflectance by the standard astronomical BVRI filters and then using the results to create color ratios, it was demonstrated that the spectral content of the specular component of the reflection varied with changes in the value of the incidence angle. The magnitude of the variation was observed to be dependent on the type of surface as well as the RMS roughness of this surface from which the reflection was measured.

Much work remains to be done in order to prove, beyond the shadow of a doubt, that the discrepancy between modelled and actual spectrometric reflectance of artificial space objects lies with the model itself. Yet, the initial findings of this study demonstrate that the hypothesis has credit and merits further investigation. On the modelling side, the reflectance model will be expanded to include consideration of the directional and uniform diffuse reflection components. However, the proposed explanation of the reddening effect will only be accepted if this phenomenon can accurately be predicted in remote spectrometric observations. Accordingly, work is progressing on the validation of a new spacecraft ground characterization procedure as well as two observational experiments to support this claim.

## 8. REFERENCES

1. *Using AMOS Telescope for Low Resolution Spectroscopy to Determine the Material Type of LEO and GEO Objects.* **Jorgensen, K., et al., et al.** s.l. : AMOS Technical Conference, Wailea, Maui, Hawaii, 2001.
2. *Remote and Ground Truth Spectral Measurement Comparisons of FORMOSAT III.* **Abercromby, K.J., et al., et al.** Maui, Hawaii : s.n., 2007. AMOS Technical Conference.
3. *Reflectance Spectra of Space Debris in GEO.* **Schildknecht, Thomas, et al., et al.** 2009. AMOS Technical Conference, Wailea, Maui, Hawaii.
4. *Obtaining material type of orbiting objects through reflectance spectroscopy measurements.* **Jorgensen, K., et al., et al.** Kihei, Maui, Hawaii : s.n., 2003. AMOS Technical Conference.
5. **Jorgensen, K.** Using Reflectance Spectroscopy to Determine Material Type of Orbital Debris. *PhD Dissertation.* Boulder, Colorado : University of Colorado, 2000.
6. *Using Space Weathering Models to Match Observed Spectra to Predicted Spectra.* **Guyote, M., Okada, J. and Abercromby, K.J.** Wailea, Maui, Hawaii : s.n., 2006. AMOS Technical Conference.
7. **Marchi, S., et al., et al.** Space weathering of near-Earth and main belt silicate-rich asteroids: observations and ion irradiation experiments. *Astronomy & Astrophysics.* 2005, Vol. 443, 3, pp. 769-775.
8. **Abercromby, Kira.** Re: Spectra reddening - Some questions. [Electronic]. Los Angeles : s.n., 09 29, 2010. Private email communication.
9. *The design and operation of the Canadian advanced nanospace eXperiment (CanX-1).* **Strass, L., et al., et al.** Toronto, Canada : s.n., 2003. Proceedings of the 21st AMSAT Space Symposium.
10. *Comparisons of Ground Truth and Remote Spectral Measurements of the FORMOSAT and ANDE Spacecraft.* **Abercromby, K.J., et al., et al.** Wailea, Maui, Hawaii : s.n., 2006. AMOS Technical Conference.
11. *A comprehensive physical model for light reflection.* **He, Xiao D., et al., et al.** 4, s.l. : ACM SIGGRAPH, July 1991, Computer Graphics, Vol. 25, pp. 175-186. ACM-0-89791436-8/91/007/0175.
12. **Pedrotti, Frank L., Pedrotti, Leno S. and Pedrotti, Leno M.** *Introduction to Optics. 3rd ed.* Upper Saddle River, NJ 07458 : Pearson Prentice Hall, 2007. 0-13-149933-5.
13. *A comparison of four BRDF models.* **Westin, Stephen H., Hongson, Li and Torrance, Kenneth E.** [ed.] H.W. Jensen and A. Keller. s.l. : Eurographics Symposium on Rendering, 2004. pp. 1-10.
14. *Interpreting asteroid spectra - Avoiding the three "Great Mistakes".* **Gaffey, M.J.** Baltimore, Maryland : s.n., 2008. Asteroid, Comets, Meteors. Vol. Poster Session II: #8162.
15. **Abercromby, K.J.** Private communication. Maui, Hawaii : s.n., September 14, 2010. This conversation was held during the 2010 AMOS Technical Conference.